

Spin dynamics of low-dimensional excitons due to acoustic phonons

A. Thilagam and M. A. Lohe

Department of Physics, The University of Adelaide, Australia 5005

E-mail: Max.Lohe@adelaide.edu.au

Abstract. We investigate the spin dynamics of excitons interacting with acoustic phonons in quantum wells, quantum wires and quantum disks by employing a multiband model based on the 4×4 Luttinger Hamiltonian. We also use the Bir-Pikus Hamiltonian to model the coupling of excitons to both longitudinal acoustic phonons and transverse acoustic phonons, thereby providing us with a realistic framework in which to determine details of the spin dynamics of excitons. We use a fractional dimensional formulation to model the excitonic wavefunctions and we demonstrate explicitly the decrease of spin relaxation time with dimensionality. Our numerical results are consistent with experimental results of spin relaxation times for various configurations of the GaS/Al_{0.3}Ga_{0.7}As material system. We find that longitudinal and transverse acoustic phonons are equally significant in processes of exciton spin relaxations involving acoustic phonons.

PACS numbers: 73.21.Fg, 72.25.Fe, 78.67.De, 73.63.Hs

1. Introduction

Excitons in low dimensional systems, formed due to the binding of electrons and holes, have well known features such as enhanced binding energies and oscillator strengths [1]. In recent years there have been increased studies of excitonic processes involving phonons within the restricted dimensional exciton energy band [2, 3], and exciton spin relaxation [4], formation and phonon-assisted thermalization [5, 6, 7] have attracted great interest. This is largely due to the significant advancement in spectroscopic techniques involving continuous-wave and time-resolved photoluminescence excitation measurements [8] which provide results of high temporal and spatial resolution. In particular, the use of polarization dependent photoluminescence [9, 10] involving circularly polarized light has extended the possible application of excitonic systems to spintronics [11, 12] in which the spin degree of freedom is exploited in electronic devices.

Several processes involving the Elliot-Yafet mechanism, the Bir-Aroniv-Pikus mechanism and the Dyakonov-Perel mechanism are known to cause spin relaxation of carriers in solids [13]. We are interested in the first of two other possible mechanisms which can cause exciton scattering involving spin- $\frac{1}{2}$ processes, firstly, holes interacting with acoustic phonons [14, 15, 16] and, secondly, long-range electron-hole exchange interactions which couple the spins of electrons and holes [17]. In narrow

well both mechanisms can become comparable, the dominant process depending on the electron density, temperature and quantum well width.

Spin dynamics of excitons are identified through measurements of circular polarization [8]–[10] in which, initially, spin polarized electrons and holes are formed followed by both spin and energy relaxation of carriers and, finally, there is recombination of carriers resulting in the measurement of a circularly polarized signal. It is not clear, however, whether the electron and hole undergo spin and energy relaxation as unlinked carriers and then become coupled (forming an exciton) after which they recombine, or whether the carriers become coupled first, then undergo spin and energy relaxation before the recombination process. Whether there is concurrence of both spin and energy relaxation in electron-hole systems also needs careful study. There have been suggestions [16] that spin relaxation occurs after energy relaxation into the excitonic ground state, while others [18] have suggested that momentum relaxation occurs simultaneously with spin relaxation in excitonic systems. This interplay of energy and spin relaxation processes needs further study in order to gain a thorough understanding of phonon related dynamics in low dimensional semiconductor systems. Such details are also vital for the accurate interpretation of experimental results.

In a simple exciton model the fourfold degeneracy at the top of the valence band, which introduces some nontrivial features in the excitonic spectrum, is neglected. The complicated nature of the multiband Wannier exciton model was noted by Dresselhaus [19] who demonstrated the absence of a well-defined exciton centre-of-mass transformation. Subsequently Baldereschi and Lipari [20, 21] studied exciton dispersion relations for a variety of semiconductor systems using a generalized centre-of-mass transformation. In the Baldereschi-Lipari approach, the "d-like" term is treated as a perturbation on the "s-like" term of the exciton Hamiltonian which has a hydrogen-like spectrum. Using this approach, Kane [22] obtained useful expressions for the energy shift of the bulk 1s exciton from the conduction band minimum. In recent years, the multiband model of the exciton interacting with phonons in bulk semiconductor systems, investigated in [23, 24], has been extended to the quasi-two dimensional model of the exciton [15, 25, 26]. These papers show that the description of low-dimensional excitons within a multiband model is a complex problem that requires extensive computational efforts. Here we use a fractional dimensional formalism to extend the study of spin dynamics of excitons to quantum wires and quantum disks and to emphasize the significance of the effect of dimensionality in the spin dynamics of excitons.

The paper is organized as follows. In Section 2 we present the theoretical formulation of the quasi-two dimensional exciton model that is used to obtain suitable dispersion relations as well as an explicit form of the exciton wavevector. In Section 3 we give details of the fractional dimensional approach and present results specific to the quantum wire system. In Section 4 we use the Bir-Pikus Hamiltonian to model the coupling of excitons to acoustic phonons and obtain expressions of matrix elements corresponding to longitudinal acoustic (LA) and transverse acoustic (TA) phonon modes. In Section 5 we extend the theory developed in Sections 2 and 4 to obtain expressions of spin transitions corresponding to the decay of heavy- and light-hole excitons and intraband as well as interband scattering in constrained systems. We report and discuss the results of salient features of excitonic processes mediated by LA and TA phonons in Section 6, and summarize our conclusions in Section 7.

2. Theoretical Formulation

We investigate properties of Wannier excitons in quantum wells fabricated using direct-gap cubic semiconductors, using as an example GaAs which is representative of a large class of III-V and II-VI zinc blende semiconductors. The conduction band edge in such systems involves an s-type spin degenerate carrier state while the valence band edge involves a p-symmetry state with a sixfold degeneracy [2, 27]. When spin-orbit interactions are included the sixfold degenerate level Γ_5 splits into a fourfold degenerate state Γ_8 (with $J = \frac{3}{2}$) and a twofold degenerate state Γ_7 ($J = \frac{1}{2}$). We neglect the twofold degenerate state, also known as the split-off band, in this paper. When analysing these spin states, we use a basis that is oriented relative to the quantization axis, where the Z-axis is chosen in the growth direction of the quantum well structure. The choice of a preferential axis of quantization for the hole spin subsequently leads to notable anisotropic properties of the exciton as we show later in this work.

The vectors in the angular momentum basis generated by $\mathbf{J} = (J_x; J_y; J_z)$ projected on the quantization axis are labelled by the magnetic quantum numbers $m = \frac{3}{2}$ for the heavy hole (HH) states and $m = \frac{1}{2}$ for the light-hole (LH) states, for the degenerate level Γ_8 (see Chapter 3 in [3]). The broken translational symmetry in the growth direction of quantum wells lifts the degeneracy of the heavy and light-hole valence bands at the Γ -point, giving rise to a distinct splitting at the two-dimensional in-plane hole wavevector $k_h = 0$. This is the basis of the formation of heavy- and light-hole excitons in quantum wells. At $k_h \neq 0$, the LH and HH states mix and hybridize giving rise to strong nonparabolicity [29, 30] in the valence band spectrum. Due to the distortion of the valence band structure, we classify the heavy- and light-hole exciton bands by their basis functions at $k_h = 0$. Unlike the split-off band which arises from the spin-orbit coupling, the splitting between the heavy-hole and light-hole states is a consequence of strain due to confinement in the growth direction. Throughout this paper k_e (k_h) marked with an arrow denotes the in-plane electron (hole) wavevector, while k_e (k_h) denotes the three-dimensional electron (hole) wavevector.

In order to define operators associated with the spins of charge carriers in quantum wells we use the standard rotation matrix $D(\alpha; \beta; \gamma)$, which is a function of the Euler angles (where $0 \leq \alpha \leq 2\pi$; $0 \leq \beta \leq \pi$; $0 \leq \gamma \leq 2\pi$), and is given by [1, 32]:

$$D(\alpha; \beta; \gamma) = \exp(-iJ_z\alpha)\exp(-iJ_y\beta)\exp(-iJ_z\gamma):$$

The angles α and β are in fact the polar angles of the spin state $\hat{J}(\alpha; \beta)$ with respect to the frame in which Z is the quantization axis. A rotated spin state can be represented as a combination of the $2J + 1$ component states using standard rotation matrices:

$$D(\alpha; \beta; \gamma) |j m\rangle = \sum_{m'} h_{j m' m}^J D(\alpha; \beta; \gamma) |j m'\rangle \quad (1)$$

The matrix elements $D_{m' m}^J(\alpha; \beta; \gamma) = h_{j m' m}^J D(\alpha; \beta; \gamma) |j m'\rangle$, where $J \geq m$; $m' \geq J$, may be written out explicitly for any J, however we require only the explicit form and transformation properties for angular momentum values $J = \frac{1}{2}$ and $J = \frac{3}{2}$ which are applicable to the electron and hole. Details are given by Brink and Satchler [32]. As the basis vectors of the representation in equation (1) are chosen as the eigenfunctions of J_z , we use the simplification $D_{m' m}^J(\alpha; \beta; \gamma) = d_{m' m}^J(\beta) e^{i m' \alpha} e^{i m \gamma}$ where d^J is the reduced rotation matrix. A variety of relations among the matrix elements $d_{m' m}^J(\beta)$ is given in Chapter 3 of the monograph by Biedenharn and Louck [33].

2.1. Electron and hole operators with arbitrary spin orientation.

By using properties of the reduced rotation matrices we are able to write the quasi-two dimensional electron and heavy- (or light-hole) creation operators as linear combinations of operators corresponding to the spin projections on the quantization axis. The creation operators of the electron $\hat{a}_{\mathbf{k}_e}^Y(\&)$, heavy hole $\hat{c}_{\mathbf{k}_h}^Y(\)$ and light-hole $\hat{c}_{\mathbf{k}_h}^Y(\)$ spinor systems thus appear as follows:

$$\begin{aligned}\hat{a}_{\mathbf{k}_e}^Y(\&) &= \sum_{\mathbf{z}} d_{\&\frac{1}{2}\mathbf{z}}^{1=2}(\mathbf{e}) \hat{a}_{\mathbf{k}_e}^Y(\mathbf{z}); \\ \hat{c}_{\mathbf{k}_h;H}^Y(\) &= \sum_{\mathbf{z}} d_{\frac{3}{2}\mathbf{z}}^{3=2}(\mathbf{h}) \hat{c}_{\mathbf{k}_h}^Y(\mathbf{z}); \\ \hat{c}_{\mathbf{k}_h;L}^Y(\) &= \sum_{\mathbf{z}} d_{\frac{1}{2}\mathbf{z}}^{3=2}(\mathbf{h}) \hat{c}_{\mathbf{k}_h}^Y(\mathbf{z})\end{aligned}\quad (2)$$

where $\mathbf{z} = \frac{1}{2}$ and $\mathbf{z} = \frac{3}{2}(\frac{1}{2})$ are the respective electron and heavy (light-) hole spin projection eigenvalues of J_z . The indices $\& =$ and $=$ denote the two possible degenerate states of the electron (at $\mathbf{k}_e = 0$) and heavy and light-holes (at $\mathbf{k}_h = 0$) respectively, and $\mathbf{e}(\mathbf{h})$ denotes the azimuthal angle of spin states of the electron (hole) operators with the in-plane wave vector $\mathbf{k}_e(\mathbf{k}_h)$. For simplicity, we use the same notation for the heavy- and light-hole wavevectors and the corresponding azimuthal angles.

The dependence of the operators $\hat{a}_{\mathbf{k}_e}^Y(\&)$, $\hat{c}_{\mathbf{k}_h;H}^Y(\)$ and $\hat{c}_{\mathbf{k}_h;L}^Y(\)$ on their respective azimuthal angles yields the expected relations at selected angles. For instance, $\mathbf{e} = 0$ yields the relations: $\hat{a}_{\mathbf{k}_e}^Y(+)=\hat{a}_{\mathbf{k}_e}^Y(\frac{1}{2})$ and $\hat{a}_{\mathbf{k}_e}^Y(\)=\hat{a}_{\mathbf{k}_e}^Y(-\frac{1}{2})$. Likewise $\mathbf{e} = \frac{\pi}{2}$ yields the relations: $\hat{a}_{\mathbf{k}_e}^Y(+)=\hat{a}_{\mathbf{k}_e}^Y(-\frac{1}{2})$ and $\hat{a}_{\mathbf{k}_e}^Y(\)=\hat{a}_{\mathbf{k}_e}^Y(\frac{1}{2})$. Similar relations can be obtained for the two types of hole spinor systems.

2.2. Exciton Wavefunction and Spin

The field operator $\hat{\Psi}^Y$ of an exciton, with a centre of mass that moves freely, is composed of electron and hole operators with spins aligned along the quantization axis, and has the expression:

$$\begin{aligned}\hat{\Psi}^Y(\mathbf{r}_e; \mathbf{r}_h) &= \sum_{\mathbf{k}_e, \mathbf{k}_h} \sum_{\mathbf{z}} \hat{c}_{\mathbf{k}_h}^Y(\mathbf{z}_h) e^{i\mathbf{k}_h \cdot \mathbf{r}_h} \sum_{\mathbf{z}} u_{\mathbf{k}_e}^{\mathbf{z}}(\mathbf{r}_e) \hat{a}_{\mathbf{k}_e}^Y(\mathbf{z}) \hat{a}_{\mathbf{k}_e}^Y(\mathbf{z}) \\ &+ \sum_{\mathbf{k}_h} \sum_{\mathbf{z}} \hat{c}_{\mathbf{k}_h}^Y(\mathbf{z}_h) e^{i\mathbf{k}_h \cdot \mathbf{r}_h} \sum_{\mathbf{z}} u_{\mathbf{k}_h}^{\mathbf{z}}(\mathbf{r}_h) \hat{c}_{\mathbf{k}_h}^Y(\mathbf{z}) \hat{c}_{\mathbf{k}_h}^Y(\mathbf{z}) ;\end{aligned}\quad (3)$$

where $\mathbf{r}_e = (x_e; y_e; z_e)$ and $\mathbf{r}_h = (x_h; y_h; z_h)$ denote the space coordinates of the electron and hole, respectively, and \mathbf{r}_e (or \mathbf{r}_h) marked with an arrow denotes the in-plane coordinates of the electron (or hole). $u_{\mathbf{k}_e}^{\mathbf{z}}(\mathbf{r}_e)$ ($u_{\mathbf{k}_h}^{\mathbf{z}}(\mathbf{r}_h)$) is the periodic component of the bulk Bloch function of the electron (hole) which depends on the projection $\mathbf{z}(\mathbf{z})$ of the spin momentum onto the positive Z-axis. As usual we assume that the Bloch functions are identical in both well and barrier materials. The conduction and valence bands in semiconductor with zinc blende structures are made up from s- and p-type atomic functions respectively. Denoting now by j the orbital

component of the s-type Bloch functions, we write the electron Bloch wavefunctions as:

$$\begin{aligned} u_{k_e}^{1=2}(r_e) &= \frac{1}{\sqrt{2}}; \frac{1}{2}i = \frac{1}{\sqrt{2}} \uparrow i; \\ u_{k_e}^{1=2}(r_e) &= \frac{1}{\sqrt{2}}; -\frac{1}{2}i = \frac{1}{\sqrt{2}} \downarrow i; \end{aligned} \quad (4)$$

where as usual \uparrow, \downarrow denote spin-up and spin-down states. Likewise, by denoting the Bloch functions with the symmetry of p_x , p_y , and p_z orbitals as X_i , Y_i , and Z_i , respectively, we may write the hole Bloch wavefunctions as linear combinations of $j(X + iY)\uparrow i$, $j(X + iY)\downarrow i$, $j(X - iY)\uparrow i$, $j(X - iY)\downarrow i$, $jZ\uparrow i$ and $jZ\downarrow i$.

It is well known that the conservation of the in-plane wavevectors k_h and k_e in quantum wells allows the lateral motion of the charge carriers to be decoupled from their motion along the Z -axis. This gives rise to subbands of quantized envelope functions, $\kappa_e(z_e)$ and $\kappa_h(z_h)$, in the conduction and valence bands respectively. The electron subband function which has even or odd parity under z_e inversion is determined by using the eigenfunction of the BenDaniel-Duke model [34] in which the potential is approximated using a finite square well. The boundary conditions at the interfaces are determined by using the wavefunction and current continuity relations and

$$\kappa_e(z_e) = \sum_{j=\frac{1}{2}}^{\infty} e^{i z_e} \kappa_{e,j}(z_e); \quad (5)$$

where $\kappa_e = (k_e; e)$.

Calculation of the hole envelope function $\kappa_h(z_h)$ is not as straight forward, as its dependence on k_h and spin components s_z gives rise to a complicated warping of the various valence subbands [30]. The axial approximation, in which a cylindrical symmetry around the crystal growth direction is assumed (following [15]), simplifies the hole subband states which may be expressed as a superposition of four states of the valence band top with spin projections $s_z = \frac{3}{2}; \frac{1}{2}; -\frac{1}{2}; -\frac{3}{2}$:

$$\kappa_h(z_h) = \sum_{j=\frac{3}{2}}^{\infty} e^{i z_h} \kappa_{h,j}(z_h) \quad (6)$$

where $\kappa_h = (k_h; h)$. Further details of the evaluation of the hole wavefunctions, characterized by the Luttinger parameters $\gamma_1; \gamma_2$ and γ_3 , are given in the Appendix.

An exciton carrying a centre-of-mass momentum K is also characterized by its spin S and its projection S_z on the quantization axis. A given exciton spin state depends on the spin-spin correlations which exist between the electron and hole spinor systems. We consider only the 1s exciton so that the exciton spin S is determined by the group theoretical rules of angular momentum vector addition. Thus the four-dimensional state space of the exciton system spanned by the states \mathcal{B}_i is characterized by a coupled system comprising the two-dimensional electron ($j_z i$) and hole ($j_z i$) spin states. In this paper we choose the exciton basis states with respect to the same axis of quantization as that of the hole and electron.

We define a generalized exciton as one that involves the coupling of an electron with wavevector k_e and spin orientation angle θ_e to a heavy- or light-hole with wavevector k_h and spin orientation angle θ_h . At low densities the exciton creation and annihilation operators satisfy boson commutation relations, but at higher densities we

write the exciton eigenvector $\mathcal{K}; S; i$ explicitly as a linear combination of all products of possible pairs of electron and hole eigenvectors:

$$\mathcal{K}; S; i = \sum_{\mathbf{k}_e, \mathbf{k}_h} F_H(\mathbf{k}_e, \mathbf{k}_h; S) \mathcal{K}_e; \mathbf{k}_h; S; i_H + \sum_{\mathbf{k}_e, \mathbf{k}_h} F_L(\mathbf{k}_e, \mathbf{k}_h; S) \mathcal{K}_e; \mathbf{k}_h; S; i_L \quad (7)$$

where $F_H(\mathbf{k}_e, \mathbf{k}_h; S)$ ($F_L(\mathbf{k}_e, \mathbf{k}_h; S)$) represents the coefficient function of coupling between the electron and heavy-hole (light-hole). We have omitted the azimuthal angles θ_e and θ_h of the spin states in equation (7), for simplicity in notation. The eigenvectors $\mathcal{K}_e; \mathbf{k}_h; S; i_H$ and $\mathcal{K}_e; \mathbf{k}_h; S; i_L$ are constructed from linear combinations of the electron and hole creation operators of the respective forms: $\hat{a}_{\mathbf{k}_e}^Y(\theta_e) \hat{c}_{\mathbf{k}_h; H}^Y(\theta_h) |0\rangle$ and $\hat{a}_{\mathbf{k}_e}^Y(\theta_e) \hat{c}_{\mathbf{k}_h; L}^Y(\theta_h) |0\rangle$, where $|0\rangle$ is the vacuum state. We have considered only the lowest heavy-hole and light-hole exciton states and therefore neglected energy band indices in equation (7). The exciton wavevector in equation (7) contains spin mixing effects between heavy and light-hole exciton states, which forms the basis by which acoustic phonons contribute to spin relaxation processes and will be further studied in Section 4.

2.3. Exciton spin states at $\theta_e = \theta_h = 0$

At $\theta_e = \theta_h = 0$ the electron and hole spins are oriented in the direction of the quantization axis and specific forms for the electron and hole creation operators are given by the following, firstly for heavy-hole excitons:

$$\mathcal{K}_e; \mathbf{k}_h; S; i_H = \sum_{\mathbf{k}_e, \mathbf{k}_h} \left(\frac{1}{2} \mathbf{k}_e; \frac{3}{2} \mathbf{k}_h \right) S_z \hat{a}_{\mathbf{k}_e}^Y(\theta_e) \hat{c}_{\mathbf{k}_h; H}^Y(\theta_h) |0\rangle \quad (8)$$

and, secondly, for light-hole excitons:

$$\mathcal{K}_e; \mathbf{k}_h; S; i_L = \sum_{\mathbf{k}_e, \mathbf{k}_h} \left(\frac{1}{2} \mathbf{k}_e; \frac{1}{2} \mathbf{k}_h \right) S_z \hat{a}_{\mathbf{k}_e}^Y(\theta_e) \hat{c}_{\mathbf{k}_h; L}^Y(\theta_h) |0\rangle; \quad (9)$$

where $|0\rangle$ is the electronic vacuum state of the system representing completely filled valence band and empty conduction bands, and the factors $\left(\frac{1}{2} \mathbf{k}_e; \frac{3}{2} \mathbf{k}_h \right) S_z$ and $\left(\frac{1}{2} \mathbf{k}_e; \frac{1}{2} \mathbf{k}_h \right) S_z$ are Clebsch-Gordon coefficients. By using equations (8) and (9) we obtain the following exciton spin states (for $S = 0$ and $S = 1$) at $\theta_e = \theta_h = 0$:

$$\mathcal{K}_e; \mathbf{k}_h; S = 0; i_L = \frac{1}{\sqrt{2}} \sum_{\mathbf{k}_e, \mathbf{k}_h} \left(\frac{1}{2} \mathbf{k}_e; \frac{1}{2} \mathbf{k}_h \right) \hat{a}_{\mathbf{k}_e}^Y(\theta_e) \hat{c}_{\mathbf{k}_h; L}^Y(\theta_h) |0\rangle \quad (10)$$

$$\begin{aligned} \mathcal{K}_e; \mathbf{k}_h; S = 1; i_L = & \frac{1}{\sqrt{6}} \sum_{\mathbf{k}_e, \mathbf{k}_h} \left(\frac{1}{2} \mathbf{k}_e; \frac{1}{2} \mathbf{k}_h \right) \hat{a}_{\mathbf{k}_e}^Y(\theta_e) \hat{c}_{\mathbf{k}_h; L}^Y(\theta_h) |0\rangle \\ & + \frac{1}{\sqrt{3}} \sum_{\mathbf{k}_e, \mathbf{k}_h} \left(\frac{1}{2} \mathbf{k}_e; \frac{3}{2} \mathbf{k}_h \right) \hat{a}_{\mathbf{k}_e}^Y(\theta_e) \hat{c}_{\mathbf{k}_h; L}^Y(\theta_h) |0\rangle; \end{aligned} \quad (11)$$

$$\mathcal{K}_e; \mathbf{k}_h; S = 1; i_H = \frac{1}{\sqrt{2}} \sum_{\mathbf{k}_e, \mathbf{k}_h} \left(\frac{1}{2} \mathbf{k}_e; \frac{3}{2} \mathbf{k}_h \right) \hat{a}_{\mathbf{k}_e}^Y(\theta_e) \hat{c}_{\mathbf{k}_h; H}^Y(\theta_h) |0\rangle; \quad (12)$$

The $S = 0$ spin state of the exciton arises from the coupling of the electron to the light-hole while the $S = 1$ spin state results from the combination of three symmetrical spin functions of the electron and light-hole spin states with the spin components $S_z = +1; 0; -1$. The $S = 1$ exciton can also be formed by coupling the components

$S_z = \pm 1$ between electron and heavy-hole spin states. Spin states $S = 2$ of the heavy-hole exciton cannot couple to photons in the light field and are therefore known as optically inactive dark excitons. Hence, the light-hole and heavy-hole excitons are characterized by the spin projections $S_z = 0; \pm 1$ and $S_z = \pm 1; \pm 2$ of the total angular momentum $S = 1; 2$ respectively. The short range exchange interaction (given below in equation (18)) further splits the ground states of both LH and HH excitons into doublet states, an effect also known as singlet-triplet splitting (see [35] for a recent review). Hence, in low dimensional systems spin mixing effects between heavy- and light-hole states result in a complicated energy spectrum and the spin states for $S = 0$ or $S = 1$ are no longer eigenfunctions of the corresponding Hamiltonian. In this paper we neglect heavy-hole and light-hole mixing effects due to exchange interactions. We also assume that the mutual conversion between the heavy-hole and light-hole exciton states arises from the phonon scattering processes as discussed in detail below in §4.

2.4. Exciton eigenvalue problem

The exciton eigenvalue $E_{\text{ex}}(\mathbf{k}; S)$ corresponding to the eigenvector $|\mathbf{k}; S\rangle$ in equation (7) is found by solving the Schrodinger equation:

$$\hat{H}_{\text{kin}} + \hat{H}_{\text{loc}} + \hat{H}_{\text{int}}^{\text{C}} + \hat{H}_{\text{int}}^{\text{exch}} |\mathbf{k}; S\rangle = E_{\text{ex}}(\mathbf{k}; S) |\mathbf{k}; S\rangle; \quad (13)$$

where the Hamiltonian is written as a sum of four terms which we now describe in turn. \hat{H}_{kin} is the kinetic energy:

$$\hat{H}_{\text{kin}} = \sum_{\mathbf{k}_e, \mathbf{k}_h} E_g - \frac{\hbar^2 \mathbf{k}_e^2}{2m_e} a_{\mathbf{k}_e}^\dagger(\mathbf{k}) a_{\mathbf{k}_e}(\mathbf{k}) - \frac{\hbar^2 \mathbf{k}_h^2}{2m_L} c_{\mathbf{k}_h, L}^\dagger(\mathbf{k}) c_{\mathbf{k}_h, L}(\mathbf{k}) + \frac{\hbar^2 \mathbf{k}_h^2}{2m_H} c_{\mathbf{k}_h, H}^\dagger(\mathbf{k}) c_{\mathbf{k}_h, H}(\mathbf{k}); \quad (14)$$

where m_e is the effective electron mass and m_H (m_L) is the heavy-hole (light-hole) mass.

\hat{H}_{loc} is associated with the localization energies of electron and hole, and is given by

$$\hat{H}_{\text{loc}} = \frac{\hbar p_{ze}^2}{2m_e} a_{\mathbf{k}_e}^\dagger(\mathbf{k}) a_{\mathbf{k}_e}(\mathbf{k}) + \frac{\hbar p_{zh}^2}{2m_L} c_{\mathbf{k}_h, L}^\dagger(\mathbf{k}) c_{\mathbf{k}_h, L}(\mathbf{k}) + \frac{\hbar p_{zh}^2}{2m_H} c_{\mathbf{k}_h, H}^\dagger(\mathbf{k}) c_{\mathbf{k}_h, H}(\mathbf{k}); \quad (15)$$

where

$$\hbar p_{ze}^2 = \int_{-L_w/2}^{L_w/2} dz_e \nabla_{\mathbf{k}_e}^2 \psi_e(z_e) \psi_e^*(z_e); \quad (16)$$

with a similar expression for $\hbar p_{zh}^2$, and L_w denotes the thickness of the quantum well.

$\hat{H}_{\text{int}}^{\text{C}}$ denotes the Hamiltonian due to the Coulomb interaction which scatters an electron in the initial state with momentum \mathbf{k} and spin \mathbf{s} to a final state with momentum $\mathbf{k} + \mathbf{q}$ and spin \mathbf{s}' . Likewise a hole in its initial state with momentum \mathbf{k}^0 and spin \mathbf{s}^0 is scattered to a final state with momentum $\mathbf{k}^0 - \mathbf{q}$ and spin \mathbf{s}'^0 , and hence:

$$\hat{H}_{\text{int}}^{\text{C}} = \frac{1}{2} \sum_{\mathbf{k}, \mathbf{s}; \mathbf{k}^0, \mathbf{s}^0} \sum_{\mathbf{q}, \mathbf{s}'; \mathbf{q}^0, \mathbf{s}'^0} V(\mathbf{q}) a_{\mathbf{k}+\mathbf{q}}^\dagger(\mathbf{s}') c_{\mathbf{k}^0-\mathbf{q}}^\dagger(\mathbf{s}'^0) c_{\mathbf{k}}(\mathbf{s}) a_{\mathbf{k}^0}(\mathbf{s}^0); \quad (17)$$

$$a_{\mathbf{k}+\mathbf{q}}^\dagger(\mathbf{s}') c_{\mathbf{k}^0-\mathbf{q}}^\dagger(\mathbf{s}'^0) c_{\mathbf{k}}(\mathbf{s}) a_{\mathbf{k}^0}(\mathbf{s}^0)$$

where

$$U(\mathbf{r}_e - \mathbf{r}_h) = \frac{e^2}{\epsilon \epsilon_0 |\mathbf{r}_e - \mathbf{r}_h|};$$

in which ϵ is the relative dielectric constant and X denotes either the heavy-hole operator H or the light-hole operator L . In the two-particle interaction matrix element

$$\langle \mathbf{K} + \mathbf{q}; \&^0; \mathbf{K}^0 - \mathbf{q}; ^0 | U(\mathbf{r}_e - \mathbf{r}_h) | \mathbf{K}^0; \&^0; \mathbf{K}; \&^0 \rangle;$$

the states to the right of the scattering potential $U(\mathbf{r}_e - \mathbf{r}_h)$ represent the initial states while those to the left represent the final scattered states.

$\hat{H}_{\text{int}}^{\text{exch}}$ denotes the Hamiltonian due to the exchange interaction which scatters an electron with spin $\&$ and momentum \mathbf{K}^0 in the conduction band to a hole state carrying momentum $\mathbf{K}^0 - \mathbf{q}$ and spin $\&$ in the valence band. At the same time, a hole state with momentum \mathbf{K} and $\&$ in the valence band is scattered to an electron state with momentum $\mathbf{K} + \mathbf{q}$ and spin $\&$ in the conduction band:

$$\hat{H}_{\text{int}}^{\text{exch}} = \frac{1}{2} \sum_{\mathbf{K}; \mathbf{K}^0; \mathbf{q}; \&^0; \&} \langle \mathbf{K}^0 - \mathbf{q}; \&^0; \mathbf{K} + \mathbf{q}; \& | U(\mathbf{r}_e - \mathbf{r}_h) | \mathbf{K}; \&^0; \mathbf{K}^0; \& \rangle \quad (18)$$

$$c_{\mathbf{K}^0 - \mathbf{q}; \&^0}^Y () a_{\mathbf{K} + \mathbf{q}; \&}^Y () c_{\mathbf{K}; \&^0} () a_{\mathbf{K}^0; \&} () :$$

By using equations (2,5-14,17,18) and by setting $\epsilon_e = \epsilon_h = 0$ we obtain, after some manipulation, the following two coupled equations for the unknown coefficient functions $F_H(\mathbf{K}; \mathbf{K}^0; \&^0; \&)$ and $F_L(\mathbf{K}; \mathbf{K}^0; \&^0; \&)$ which are defined by equation (7):

$$0 = E_e(\mathbf{K}_e) + E_H(\mathbf{K}_h) - E_{\text{ex}}^H(\mathbf{K}) - F_H(\mathbf{K}; \mathbf{K}^0; \&^0; \&) \quad (19)$$

$$+ \sum_{\mathbf{Z}} \int_{\mathbf{z}; \mathbf{z}} d\mathbf{K}^0 V_C(\mathbf{K}; \mathbf{K}^0; H) (1 - S) V_{\text{exch}}(\mathbf{K}; \mathbf{K}^0; H)$$

$$F_H(\mathbf{K}; \mathbf{K}^0; \&^0; \&) d_{\& \frac{1}{2}}^{1=2}(\mathbf{z}) d_{\frac{3}{2}}^{3=2}(\mathbf{z}) + F_L(\mathbf{K}; \mathbf{K}^0; \&^0; \&) d_{\& \frac{1}{2}}^{1=2}(\mathbf{z}) d_{\frac{3}{2}}^{3=2}(\mathbf{z})$$

and

$$0 = E_e(\mathbf{K}_e) + E_L(\mathbf{K}_h) - E_{\text{ex}}^L(\mathbf{K}) - F_L(\mathbf{K}; \mathbf{K}^0; \&^0; \&) \quad (20)$$

$$+ \sum_{\mathbf{Z}} \int_{\mathbf{z}; \mathbf{z}} d\mathbf{K}^0 V_C(\mathbf{K}; \mathbf{K}^0; L) (1 - S) V_{\text{exch}}(\mathbf{K}; \mathbf{K}^0; L)$$

$$F_H(\mathbf{K}; \mathbf{K}^0; \&^0; \&) d_{\& \frac{1}{2}}^{1=2}(\mathbf{z}) d_{\frac{3}{2}}^{3=2}(\mathbf{z}) + F_L(\mathbf{K}; \mathbf{K}^0; \&^0; \&) d_{\& \frac{1}{2}}^{1=2}(\mathbf{z}) d_{\frac{3}{2}}^{3=2}(\mathbf{z}) ;$$

where $E_e(\mathbf{K}_e)$ and $E_H(\mathbf{K}_h)$ ($E_L(\mathbf{K}_h)$) denote the in-plane energies of the electron and heavy-hole (light-hole) respectively, and $E_{\text{ex}}^H(\mathbf{K})$ ($E_{\text{ex}}^L(\mathbf{K})$) denotes the heavy-hole (light-hole) exciton energy in the plane of the quantum well. The angles ϵ_e and ϵ_h are defined by equations (5) and (6).

The integral forms of $V_C(\mathbf{K}; \mathbf{K}^0; X)$ and $V_{\text{exch}}(\mathbf{K}; \mathbf{K}^0; X)$ which are the in-plane Fourier transforms of the Coulomb potential, with $X = H$ ($\mathbf{z}; \frac{0}{z} = \frac{3}{2}$) or $X = L$ ($\mathbf{z}; \frac{0}{z} = \frac{1}{2}$), are given by:

$$V_C(\mathbf{K}; \mathbf{K}^0; X) = \frac{e^2}{2} \frac{1}{\mathbf{K} - \mathbf{K}^0} \sum_{\mathbf{Z}} \int_{\mathbf{z}; \mathbf{z}} e^{i(\mathbf{z} - \mathbf{h} - \frac{0}{z} - \frac{0}{h})} \quad (21)$$

$$dz_e dz_h e^{-i\mathbf{K}^0 \cdot \mathbf{z}_e - i\mathbf{K} \cdot \mathbf{z}_h} \int_{\mathbf{K} + \mathbf{q}; \&^0}^{\mathbf{K}^0; \&} (z_e) \int_{\mathbf{K}^0; \&^0}^{\mathbf{K} + \mathbf{q}; \&} (z_h) \int_{\mathbf{K}; \&^0}^{\mathbf{K}^0; \&} (z_e) \int_{\mathbf{K}^0; \&^0}^{\mathbf{K} + \mathbf{q}; \&} (z_h);$$

and

$$V_{\text{exch}}(\mathbf{K}; \mathbf{K}^0; X) = \frac{e^2}{2} \frac{1}{\mathbf{K} \cdot \mathbf{K}^0} \sum_{\mathbf{z}; \frac{0}{\mathbf{z}}}^X e^{i(\mathbf{z} \cdot \mathbf{h} - \frac{0}{\mathbf{z}} \cdot \frac{0}{\mathbf{h}})} \quad (22)$$

$$dz_e dz_h e^{i\mathbf{K} \cdot \mathbf{K}^0} \tilde{\chi}_e(\mathbf{z}_e) \tilde{\chi}_h(\mathbf{z}_h) \tilde{\chi}_e(\mathbf{K} + \mathbf{q}^0) \tilde{\chi}_h(\mathbf{K}^0 - \mathbf{q}^0) \tilde{\chi}_e(\mathbf{z}_e) \tilde{\chi}_h(\mathbf{z}_h):$$

Equations (19) and (20) give rise to strong nonparabolic exciton centre-of-mass dispersions and require a large basis function set and sophisticated numerical techniques in order to be solved, even for the particular case $\mathbf{z}_e = \mathbf{z}_h = 0$. As a result of the nonparabolicity there is no unique definition for the mass of the exciton, which has resulted in a range of mass values in the literature [36]. The hole spin components also become mixed and some authors [15] have found it convenient to use the parity-imp mechanism to incorporate changes in parity in the valence band states.

The centre-of-mass momentum wavevector \mathbf{K} and the relative wavevector \mathbf{K} are defined in terms of the electron and hole wavevectors (\mathbf{K}_e and \mathbf{K}_h respectively) by:

$$\mathbf{K} = \mathbf{K}_e + \mathbf{K}_h;$$

$$\mathbf{K} = (1 - \#) \mathbf{K}_e + \# \mathbf{K}_h; \quad (23)$$

where the parameter $\#$ is generally used in a scalar form [5, 36, 37] which conveniently allows the decoupling of the exciton centre-of-mass motion from its relative motion. In more rigorous calculations involving the heavy-hole and light-hole dispersion relations, $\#$ has been used as a tensor [20, 21]. Recently, Siarkos et al [25] used a variational approach involving minimization of the exciton energy and obtained optimized values of $\#$ in the range $0.6 \leq \# \leq 0.5$ at $\mathbf{K} \approx 0.4 \text{ nm}^{-1}$. For our work, we select suitable values for $\#$ for the heavy- and light-hole 1s exciton by extending the expression derived by Kane [22] for the energy shift of the bulk 1s exciton from the conduction band minimum to a low dimensional \mathbf{K} space:

$$E_{\text{ex}}^X(\mathbf{K}) = R_y - 5g_1(E) \frac{\hbar^2 \mathbf{K}^2}{2} + \frac{1}{M_a} \frac{1}{M_c};$$

$$\frac{1}{M_a} = \frac{1}{M_0} - \frac{40}{3} g_3(E) s^2 \frac{\hbar^2}{2}$$

$$\frac{1}{M_c} = \frac{2s^2}{m_0} \frac{\hbar^2}{2} \quad (24)$$

where the + sign and $X = H$ correspond to the heavy-hole exciton while the - sign and $X = L$ correspond to the light-hole exciton. R_y is the effective Rydberg constant, m_0 is the free electron mass and

$$M_0 = \frac{1}{1 + m_e}; \quad s = \frac{m_e}{1 + m_e};$$

The functions $g_1(E)$ and $g_3(E)$ given by Kane [22] are assumed to apply in low dimensional systems, and the constants $\frac{1}{2}$; $\frac{2}{3}$ are discussed in the Appendix. By using $E = R_y$ and the approximation $\frac{3}{2} \approx \frac{2}{2}$ we obtain:

$$e = \# = \frac{m_e}{1 + m_e} + 2s^2 \frac{1}{2m_e} \frac{1}{1 + m_e};$$

$$h = 1 - \#: \quad (25)$$

With the value $m_e = 0.065 m_0$ for the effective electron mass and γ_1, γ_2 as given in table 1 for the GaAs/AlGaAs material system, we obtain $\gamma_e = 0.377$ for the heavy-hole exciton and $\gamma_e = 0.116$ for the light-hole exciton. These values are consistent with those obtained in reference [25].

In order to obtain an explicit form for the exciton wavevector, we neglect the relatively weak exchange interaction term $V_{\text{exch}}(\mathbf{k}; \mathbf{k}^0; \mathbf{X})$ involving an overlap of the conduction and valence bands. We now write equation (7) in the form :

$$\mathcal{K}; S_i = \mathcal{K}; S_{iH} + \mathcal{K}; S_{iL} \quad (26)$$

and use equations (19) and (20) to obtain (for the heavy-hole exciton):

$$\begin{aligned} \mathcal{K}; S_{iH} = & \sum_{\mathbf{X}} \sum_{\mathbf{X}} d_{\frac{1}{2} z}^{1=2}(\mathbf{X}) d_{\frac{3}{2} z}^{3=2}(\mathbf{X}) \mathcal{K}; \mathbf{k}_e \mathbf{k}_h \psi_s(\mathbf{k}_e \mathbf{k}_h + \mathbf{k}_h \mathbf{k}_e) \\ & \mathbf{k}_e; \mathbf{k}_h; \mathbf{q}_z = \begin{matrix} 1; z = \frac{1}{2} \\ z = \frac{3}{2} \end{matrix} \\ & F_e(\mathbf{q}_z) F_h(\mathbf{q}_z) \hat{a}_{\mathbf{k}_e}^V(\mathbf{z}) \hat{c}_{\mathbf{k}_h}^V(\mathbf{z}) \mathcal{J}_i; \end{aligned} \quad (27)$$

and (for the light-hole exciton):

$$\begin{aligned} \mathcal{K}; S_{iL} = & \sum_{\mathbf{X}} \sum_{\mathbf{X}} d_{\frac{1}{2} z}^{1=2}(\mathbf{X}) d_{\frac{3}{2} z}^{1=2}(\mathbf{X}) \mathcal{K}; \mathbf{k}_e \mathbf{k}_h \psi_s(\mathbf{k}_e \mathbf{k}_h + \mathbf{k}_h \mathbf{k}_e) \\ & \mathbf{k}_e; \mathbf{k}_h; \mathbf{q}_z = \begin{matrix} 1; z = \frac{1}{2} \\ z = \frac{1}{2} \end{matrix} \\ & F_e(\mathbf{q}_z) F_h(\mathbf{q}_z) \hat{a}_{\mathbf{k}_e}^V(\mathbf{z}) \hat{c}_{\mathbf{k}_h}^V(\mathbf{z}) \mathcal{J}_i \end{aligned} \quad (28)$$

where θ is the angle of scattering and σ denotes the polarization state of the exciton. We have also dropped the $X = H (L)$ label from the hole creation operator as we have restricted the azimuthal angles to $\phi_e = \phi_h = 0$, and therefore use the same notation $\hat{c}_{\mathbf{k}}^V(\mathbf{z})$ for the heavy-hole and light-hole creation operator.

The form factors $F_e(\mathbf{q}_z)$ and $F_h(\mathbf{q}_z)$ are given by:

$$\begin{aligned} F_e(\mathbf{q}_z) = & \int d\mathbf{z}_e e^{i\mathbf{q}_z \cdot \mathbf{z}_e} \mathcal{K}_{ej}(\mathbf{z}_e)^2; \\ F_h(\mathbf{q}_z) = & \int d\mathbf{z}_h e^{i\mathbf{q}_z \cdot \mathbf{z}_h} \mathcal{K}_{hj}(\mathbf{z}_h)^2; \end{aligned} \quad (29)$$

The exciton wavevectors in equations (26) – (28) generalize the form used in earlier work [5] in which we assumed a simple two-band model without taking into account the fourfold degeneracies of the upper valence energy bands. $\psi_s(\mathbf{k}_e \mathbf{k}_h + \mathbf{k}_h \mathbf{k}_e)$ is the wavefunction of a hydrogen type system in momentum space, which depends on the relative electron-hole separation. This function determines the intrinsic properties of the exciton and forms the basis of the fractional dimensional approach detailed in the next section.

3. The fractional dimensional formalism

In the fractional dimensional approach the confined "exciton and quantum well", "exciton and quantum wire" or "exciton and disk" system is modelled using conventional Hilbert spaces which carry a fractional dimensional parameter, and in which the composite exciton system behaves in an unconfined manner, and so the fractional dimension is related to the degree of confinement of the physical system. Such an approach introduces simplicity and utility and has been used in the investigation of several important processes in low dimensional systems [38]–[42].

The binding energy of a fractional dimensional exciton [45] is given by:

where $n = 1; 2; \dots$ is the principal quantum number of the exciton internal state and R_y is the effective Rydberg constant. The function $\psi_{1s}(\tilde{r})$ appearing in equations (27) and (28), where $\tilde{r} = r_{eh} + r_{he}$, has been obtained (Thilagam [38]) in the form :

where a_{B} is the three-dimensional Bohr radius of the exciton. κ yields the expected forms in the exact three-dimensional and two-dimensional limits. The dimensional parameter κ characterizes the degree of "compression" of the confined exciton and can be calculated in several ways (see for instance references [45]–[47]). Once κ is determined, many useful properties (see [38]–[42], [45]) can be determined by substituting its value into the appropriate equation that corresponds to a physical quantity. Recently, Escorcia et al. [46] used variationally determined envelope functions to calculate the wavefunctions of the exciton relative motion in quantum wires and disks. Like earlier approaches [45, 47], the technique of evaluating κ in reference [46] does not include valence band coupling effects between the heavy- and light-hole bands. For our work, we improve on earlier methods [45]–[47] by utilizing realistic values of κ that is evaluated by including valence band coupling effects through a 4 × 4 Baldereschi-Lipari Hamiltonian [20, 21] which describes the relative motion of the exciton. This allows salient features due to the anisotropic exciton band model to be incorporated in .

At large R values the dimensionality of the light-hole exciton is noticeably smaller than that of the heavy-hole exciton. The dimensionalities reach minimum values at the strong confinement limit of $R_m \approx 3.5 \cdot 10^9$ m. For $R \ll R_m$ the excitonic wavefunction spreads beyond the well material and leads to a rapid increase of the dimensionalities as shown in figure 1. The effect of including the off-diagonal elements of the Luttinger Hamiltonian through the 4×4 Baldereschi-Lipari Hamiltonian [20, 21]

Fig. 1

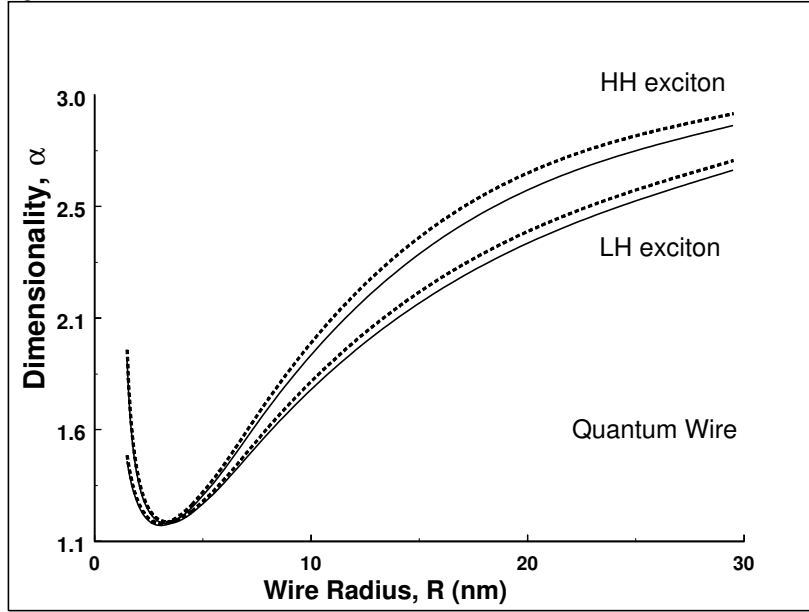


Figure 1. Dimensionalities of the heavy- and light-hole excitons as functions of the quantum wire radius R in GaAs/Al_{0.3}Ga_{0.7}As using the parameters in table 1. The dashed lines correspond to calculations in which off-diagonal elements of the 4 × 4 Bakker-Lipari Hamiltonian (references [20, 21]) are neglected.

can be seen in the difference between the solid curves and dashed curves (in which the off-diagonal elements of the 4×4 Hamiltonian are neglected). This figure shows that the ideal lower limit of $\beta = 1$ is never attained. Moreover, because $\beta > 2$ for $R > 10^{-8} \text{m}$, dimensionalities in quantum wires are not restricted to the range $1 \leq d \leq 2$. These results also indicate that it is not appropriate to use equation (30) to estimate β in quantum wires.

4. Exciton-phonon interaction

Two main mechanisms are considered when analysing exciton-phonon interactions in semiconductors: the deformation potential and the piezoelectric interaction. We write the Hamiltonian $\hat{H}_{\text{ex-ph}}^{\text{D.P.}}$ describing the exciton-phonon interaction, due to the deformation potential, in terms of electron and hole creation and annihilation operators:

$$\hat{H}_{\text{ex-ph}}^{\text{D.P.}} = \sum_{\mathbf{k}, \mathbf{q}; \mathbf{q}_z; \frac{0}{2}} \sum_{\mathbf{h}} \sum_{\mathbf{i}} M_z(\mathbf{q}; \mathbf{q}_z) \hat{a}_{\mathbf{k}+\mathbf{q}}^{\dagger}(\frac{0}{2}) \hat{a}_{\mathbf{k}}(\frac{0}{2}) + M_z(\mathbf{q}; \mathbf{q}_z) \hat{c}_{\mathbf{k}+\mathbf{q}}^{\dagger}(\frac{0}{2}) \hat{c}_{\mathbf{k}}(\frac{0}{2}) + b^{\dagger}(\mathbf{q}; \mathbf{q}_z) + b(\mathbf{q}; \mathbf{q}_z); \quad (32)$$

where the phonon wave vector is given by $\mathbf{q} = (q_x; q_y; q_z) = (\mathbf{q}; q_z)$, and where $b^{\dagger}(\mathbf{q}; \mathbf{q}_z)$ (respectively $b(\mathbf{q}; \mathbf{q}_z)$) denotes the creation (respectively annihilation) operator of a \mathbf{m} mode phonon. The \mathbf{m} mode is denoted LA for longitudinal acoustic phonons and TA for transverse acoustic phonons. The strain tensor ϵ_{ij} due to the various \mathbf{m} mode phonons is written in terms of normal mode coordinates as

$$\epsilon_{ij} = \sum_{\mathbf{q}} \frac{1}{2} \sum_{\mathbf{s}} \frac{\hbar}{2V\omega_{\mathbf{q}}} \left(b^{\dagger}(\mathbf{q}; \mathbf{q}_z) + b(\mathbf{q}; \mathbf{q}_z) \right) (\hat{e}_i q_j + \hat{e}_j q_i) e^{i\mathbf{q} \cdot \mathbf{r}}; \quad (33)$$

where ρ is the mass density of the material. The acoustic phonon energy spectrum is determined by $\omega_{\mathbf{qLA}} = v_{\text{LA}} |\mathbf{q}|$ for the longitudinal mode and $\omega_{\mathbf{qTA}} = v_{\text{TA}} |\mathbf{q}|$ for the transverse mode, with v_{LA} and v_{TA} denoting the corresponding sound velocities. The term \hat{e}_i represents the unit vector of polarization of the \mathbf{m} -phonon along the i -direction. The longitudinal mode \hat{e}_{LA} and the two transverse modes \hat{e}_{TA1} and \hat{e}_{TA2} take the form [48]:

$$\begin{aligned} \hat{e}_{\text{LA}} &= \frac{1}{|\mathbf{q}|} \begin{pmatrix} q_x \\ q_y \\ q_z \end{pmatrix}; \\ \hat{e}_{\text{TA1}} &= \frac{1}{|\mathbf{q}|} \begin{pmatrix} q_y \\ -q_x \\ 0 \end{pmatrix}; \\ \hat{e}_{\text{TA2}} &= \frac{1}{|\mathbf{q}|} \begin{pmatrix} q_x q_z \\ q_y q_z \\ q_x^2 + q_y^2 \end{pmatrix}; \end{aligned} \quad (34)$$

where the TA1-mode (TA2-mode) corresponds to the transverse phonon polarized along the x (y)-direction.

The matrix elements $M_z(\mathbf{q}; \mathbf{q}_z)$ and $M_z(\mathbf{q}; \mathbf{q}_z)$ in equation (32) depend on the precise nature of the exciton-phonon interactions, such as the deformation potential interaction, the piezoelectric interaction, and the phonon mode. We have explicitly

included the spin indices to distinguish the hole states involved in the interaction. Due to the isotropic nature of the electron related interaction with acoustic phonons in cubic III-V semiconductors [49], we obtain:

$$\begin{aligned} M_{\frac{1}{2}}^{LA}(\mathbf{q}; \mathbf{q}_z) &= \frac{\hbar \tilde{\chi}_{1j}}{2 V_{LA}} c \\ M_{\frac{1}{2}}^{TA}(\mathbf{q}; \mathbf{q}_z) &= 0; \end{aligned} \quad (35)$$

where c is the deformation potential constant associated with the conduction band. In using equation (35) some papers (for example [50]) have neglected the deformation potential coupling to the TA phonon mode. The importance of including interactions due to TA phonons becomes clear in the context of hole-phonon interactions, which we consider next.

The component of the hole related interaction in the exciton-phonon Hamiltonian is described by the Bir-Pikus Hamiltonian H_{BP} [51, 52] which takes the form

$$H_{BP} = \begin{pmatrix} 0 & F & H & I & 0 \\ F & G & 0 & I & C \\ H & 0 & G & H & A \\ I & 0 & G & H & A \\ 0 & I & H & F & 0 \end{pmatrix} \quad (36)$$

where the matrix elements are defined (following [51]) in terms of deformation potential tensor components A_{ij}^A and strain tensor components ϵ_{ij} by:

$$A = \sum_{ij} A_{ij}^A \epsilon_{ij}; \quad (A = F; G; H; I)$$

where

$$\begin{aligned} F_{11} &= F_{22} = a & F_{33} &= b; \\ G_{11} &= G_{22} = \frac{1}{3}(a + 2b) & G_{33} &= \frac{1}{3}(4a - b); \\ H_{13} &= H_{31} = ic & H_{23} &= H_{32} = i H_{13}; \\ I_{11} &= I_{22} = \frac{1}{3}(a - b) & I_{12} &= I_{21} = ic; \end{aligned} \quad (37)$$

with all other components $A_{ij}^A = 0$. The values a , b and c are evaluated using the matrix elements $\langle \hat{E}_{xx} \rangle$, $\langle \hat{E}_{yy} \rangle$ and $\langle \hat{E}_{xy} \rangle + \langle \hat{E}_{yx} \rangle$ where the tensor operator \hat{E}_{ij} is obtained [52] by subtracting elements of the Hamiltonian of the unstrained crystal from those in a strained crystal.

The effective deformation potential interaction can be obtained separately for TA and LA hole-phonon interactions via a suitable transformation of the deformation potential tensor matrix:

$$e_{i^0 j^0}^A = \sum_{ij} U_{i^0 i} U_{j^0 j} A_{ij}^A \quad (38)$$

where the matrix U is given by:

$$U = \begin{pmatrix} \bar{q}_z \cos \kappa & \bar{q}_z \sin \kappa & \bar{q}_x \\ \sin \kappa & \cos \kappa & 0 \\ \bar{q}_x \cos \kappa & \bar{q}_x \sin \kappa & \bar{q}_z \end{pmatrix} \quad (39)$$

where $\bar{q}_z = \frac{q_z}{\hbar j}$, $\bar{q}_x = \frac{q_x}{\hbar j}$ and $\kappa = (\kappa_x; \kappa_y)$.

By using equations (37), (38) and (39) we obtain expressions for the matrix elements $M_z(\mathbf{q}; \mathbf{q}_z)$ for different phonon modes :

$$\begin{aligned} M_{\frac{1}{2}(\frac{3}{2})}^{\text{LA}}(\mathbf{q}; \mathbf{q}_z) &= \frac{\hbar}{2V_{\text{LA}}} \frac{\sim \mathfrak{H}j}{S} a^0_{\frac{1}{2}(\frac{3}{2})}(\bar{\mathbf{q}}_k; \bar{\mathbf{q}}_z; \mathbf{k}) \\ M_{\frac{1}{2}(\frac{3}{2})}^{\text{TA1}}(\mathbf{q}; \mathbf{q}_z) &= \frac{\hbar}{2V_{\text{TA1}}} \frac{\sim \mathfrak{H}j}{S} b^0_{\frac{1}{2}(\frac{3}{2})}(\bar{\mathbf{q}}_k; \bar{\mathbf{q}}_z; \mathbf{k}) \\ M_{\frac{1}{2}(\frac{3}{2})}^{\text{TA2}}(\mathbf{q}; \mathbf{q}_z) &= \frac{\hbar}{2V_{\text{TA2}}} \frac{\sim \mathfrak{H}j}{S} c^0_{\frac{1}{2}(\frac{3}{2})}(\bar{\mathbf{q}}_k; \bar{\mathbf{q}}_z; \mathbf{k}) \end{aligned} \quad (40)$$

where a^0 and b^0 are obtained using a , b and c (see equation (37)) and the $+$ and $-$ signs on the right hand side of equation (40) correspond to the light- and heavy-holes respectively. i ($i = 1, 2, 3$) are explicit functions of $\bar{\mathbf{q}}_k$, $\bar{\mathbf{q}}_z$ and \mathbf{k} , and v_{TA1} and v_{TA2} are the respective sound velocities corresponding to polarization in the x and y -direction.

The Hamiltonian $\hat{H}_{\text{ex-ph}}^{\text{Piez}}$ describing the exciton-acoustic phonon scattering due to the piezoelectric effect for LA and TA phonons can be obtained using the Bir-Pikus Hamiltonian in equation (36) and the matrix U in equation (39), in the form :

$$\hat{H}_{\text{ex-ph}}^{\text{Piez}} = \sum_{\mathbf{k}, \mathbf{q}; \mathbf{q}_z; \frac{0}{2}, \frac{0}{2}} \frac{\hbar}{2} \begin{pmatrix} a^y_{\mathbf{k}+\mathbf{q}}(\mathbf{z}) & c^y_{\mathbf{k}+\mathbf{q}}(\mathbf{z}) \end{pmatrix} \begin{pmatrix} a^0_{\mathbf{k}}(\mathbf{z}) & c^0_{\mathbf{k}}(\mathbf{z}) \end{pmatrix} \begin{pmatrix} b^y(\mathbf{q}; \mathbf{q}_z) + b(\mathbf{q}; \mathbf{q}_z) \end{pmatrix} \quad (41)$$

where the matrix elements $M_p(\mathbf{q}; \mathbf{q}_z)$ are given by:

$$\begin{aligned} M_p^{\text{LA}}(\mathbf{q}; \mathbf{q}_z) &= i \frac{\hbar}{2V_{\text{LA}}} \frac{\sim \mathfrak{H}j}{S} 3eh_{14} \bar{\mathbf{q}}_k^2 \bar{\mathbf{q}}_z \sin 2\theta_k \\ M_p^{\text{TA1}}(\mathbf{q}; \mathbf{q}_z) &= i \frac{\hbar}{2V_{\text{TA1}}} \frac{\sim \mathfrak{H}j}{S} 3eh_{14} \bar{\mathbf{q}}_k (\bar{\mathbf{q}}_z^2 - \bar{\mathbf{q}}_k^2) \sin 2\theta_k \\ M_p^{\text{TA2}}(\mathbf{q}; \mathbf{q}_z) &= i \frac{\hbar}{2V_{\text{TA2}}} \frac{\sim \mathfrak{H}j}{S} 2eh_{14} \bar{\mathbf{q}}_k \bar{\mathbf{q}}_z (\cos 2\theta_k - 1) \end{aligned} \quad (42)$$

where h_{14} is the piezoelectric coupling constant. Unlike the matrix elements for the deformation potential $M_z(\mathbf{q}; \mathbf{q}_z)$, which depend on the hole spin, the elements $M_p(\mathbf{q}; \mathbf{q}_z)$ corresponding to the piezoelectric interaction are independent of the hole spin.

5. Exciton decay and scattering involving acoustic phonons

In this section we derive rates of spin transitions due, firstly, to the decay of heavy- and light-hole excitons, secondly, to intraband scattering (heavy-hole to heavy-hole, light-hole to light-hole) and, thirdly, to interband scattering (heavy-hole to light-hole, light-hole to heavy-hole) due to interactions with LA and TA phonons. For the decay process, we suppose that initially an exciton with wavevector \mathbf{K} and spin S decays into an electron-hole pair by absorbing an acoustic phonon. We assume that the

wavefunction of the final state can be written in terms of a free electron-hole pair as:

$$\langle \mathbf{K}; S | i_{\text{decay}} = \sum_{\mathbf{K}, \mathbf{K}', \mathbf{q}} \sum_{\mathbf{q}_z} \hat{a}_{\mathbf{K}}^{\dagger}(\mathbf{z}) \hat{c}_{\mathbf{K}'}^{\dagger}(\mathbf{z}) b(\mathbf{q}; \mathbf{q}_z) | i_{\mathbf{q}; \mathbf{q}_z} \rangle; \quad (43)$$

where we have included the allowed modes within the summation, although the contribution of each mode phonon interaction to the decay process can be analysed separately by excluding from the summation, and where $n_{\mathbf{q}; \mathbf{q}_z}$ denotes the occupation number of phonons.

For the scattering process, we suppose that an exciton is scattered from its initial state of wavevector \mathbf{K} and spin S to a final state with wavevector \mathbf{K}' ($\neq \mathbf{K}$) and spin S' through the following channels which may occur with or without a change of the exciton spin:

- (i) $\langle \mathbf{K}; S | i \rightarrow \langle \mathbf{K}'; S' | i$ with energy $\sim \hbar \omega_{\mathbf{K}-\mathbf{K}'; \mathbf{q}_z}$ (acoustic phonon emission),
- (ii) $\langle \mathbf{K}; S | i \rightarrow \langle \mathbf{K}'; S' | i$ with energy $\sim \hbar \omega_{\mathbf{K}'-\mathbf{K}; \mathbf{q}_z}$ (acoustic phonon absorption).

The spin relaxation time τ_{sp} is calculated using the Fermi golden rule:

$$\frac{1}{\tau_{\text{sp}}} = \frac{2}{\hbar} \sum_{\mathbf{K}, \mathbf{q}; \mathbf{q}_z} \sum_{\mathbf{K}'} | \langle \mathbf{K}'; S' | H_{\text{int}} | \mathbf{K}; S \rangle |^2 (f_{\mathbf{K}+\mathbf{q}} + 1) f_{\mathbf{K}} N_{\mathbf{q}} (E_{\text{ex}}(\mathbf{K} + \mathbf{q}) - E_{\text{ex}}(\mathbf{K}) \pm \hbar \omega_{\mathbf{q}}) + (f_{\mathbf{K}-\mathbf{q}} + 1) f_{\mathbf{K}} (N_{\mathbf{q}} + 1) (E_{\text{ex}}(\mathbf{K} - \mathbf{q}) - E_{\text{ex}}(\mathbf{K}) \pm \hbar \omega_{\mathbf{q}}); \quad (44)$$

where $|i\rangle$ and $|f\rangle$ denote the initial and final states, H_{int} is the interaction operator and $N_{\mathbf{q}}$ is the thermalised average number of phonons at the lattice temperature T_{lat} , and is given by the Bose-Einstein distribution

$$N_{\mathbf{q}} = \frac{1}{\exp\left(\frac{\hbar \omega_{\mathbf{q}}}{k_B T_{\text{lat}}}\right) - 1};$$

The exciton distribution function $f_{\mathbf{K}}$ is given by [7]:

$$f_{\mathbf{K}} = \exp\left(-\frac{E_{\text{ex}}(\mathbf{K}) - \mu}{k_B T_{\text{ex}}}\right) = \exp\left(-\frac{E_{\text{ex}}(\mathbf{K}) - \mu}{k_B T_{\text{ex}}} - \frac{2}{g m_e k_B T_{\text{ex}}} \ln \frac{n_{\text{ex}}}{n_0}\right); \quad (45)$$

where T_{ex} is the exciton temperature, k_B is the Boltzmann constant, μ is the chemical potential, n_{ex} is the exciton density, n_0 is defined in equation (25), g is the spin degeneracy factor [7] and, as before, m_e is the effective electron mass. The summation in equation (44) includes all the initial and final spin states of the coupled electron-hole system and thus the relaxation time τ_{sp} incorporates the effect of changes from spin-up (spin-down) to spin-down (spin-up) electron and hole states of the exciton.

By using the initial state given by equation (26), the final state given by equation (43), and the Hamiltonian operator of exciton-phonon interactions due to the deformation potential in equation (32), we obtain the transition matrix elements for the decay of a heavy-hole exciton into a free electron heavy-hole pair as:

$$\begin{aligned} \langle \mathbf{K}; S | i_{\text{decay}}^{\text{DP}} | \mathbf{K}'; S' \rangle &= \sum_{\mathbf{z}} \sum_{\mathbf{q}; \mathbf{q}_z} F_e(\mathbf{q}_z) \langle \mathbf{K}'; S' | \hat{H}_{\text{int}}^{\text{DP}} | \mathbf{K}; S \rangle \\ &= \sum_{\mathbf{z}} \sum_{\mathbf{q}; \mathbf{q}_z} F_e(\mathbf{q}_z) \langle \mathbf{K}'; S' | \hat{H}_{\text{int}}^{\text{DP}} | \mathbf{K}; S \rangle \\ &= \sum_{\mathbf{z}} \sum_{\mathbf{q}; \mathbf{q}_z} F_e(\mathbf{q}_z) \langle \mathbf{K}'; S' | \hat{H}_{\text{int}}^{\text{DP}} | \mathbf{K}; S \rangle \\ &= \sum_{\mathbf{z}} \sum_{\mathbf{q}; \mathbf{q}_z} F_e(\mathbf{q}_z) \langle \mathbf{K}'; S' | \hat{H}_{\text{int}}^{\text{DP}} | \mathbf{K}; S \rangle \end{aligned} \quad (46)$$

By using equation (41), we obtain the transition matrix elements for the decay of the heavy-hole exciton due to piezoelectric effect as:

$$\text{hf } \hat{H}_{\text{ex ph}}^{\text{piez}} \hat{H}_{\text{decay}}^{\text{HH}} = M_P(\mathbf{q}; \mathbf{q}_L) \frac{1}{q} \frac{1}{(f_{\mathbf{k}_q} + 1) f_{\mathbf{k}_q} (N_q + 1/2)}$$

The transition matrix elements corresponding to the scattering of a heavy-hole exciton to another heavy-hole state due to deformation potential interaction is obtained as:

$$\text{as:} \quad \text{hf} \overset{\text{D P}}{\underset{\text{ex ph}}{\text{f}}} \overset{\text{H H}}{\underset{\text{scatt}}{\text{f}}} \overset{\text{D P}}{\text{}} = \frac{X}{M} \frac{h}{z} \frac{(\mathbf{q}; \mathbf{q}_z) F_e(\mathbf{q}_z) F_e(\mathbf{q}_z^0)}{\mathbf{k}; \mathbf{q}_z^0} \frac{1_s(\mathbf{h} \mathbf{K} - \mathbf{K})}{1_s(\mathbf{h} \mathbf{K}^0 - \mathbf{K})} \frac{i}{\frac{1}{2} \frac{1}{2} (\mathbf{q}; \mathbf{q}_z) F_h(\mathbf{q}_z) F_h(\mathbf{q}_z^0)} \frac{1_s(\mathbf{h} \mathbf{K}^0 + \mathbf{K} - \mathbf{q})}{1_s(\mathbf{h} \mathbf{K} + \mathbf{K})} \frac{q}{d^{\frac{1}{2}} \frac{1}{2} (\mathbf{q}; \mathbf{q}_z) d^{\frac{3}{2}} \frac{1}{2} (\mathbf{q}; \mathbf{q}_z) K^0} \frac{1}{(f_K(\mathbf{q} + 1) f_K(\mathbf{N}_q + 1; 1))} \quad (47)$$

The spin relaxation rates for various phonon mediated processes (such as those due to the deformation potential and piezoelectric interactions), are usually calculated using equations (46)-(47) in (44) and by using the following summation over spin states (see Brink [32], page 24):

$$\begin{aligned} X_{0=1}^{\frac{1}{2}} d_{\frac{1}{2} \quad 0 \frac{1}{2}}^{1=2}(\quad)^2 &= 2 \\ X_{0=1}^{\frac{3}{2}} d_{\frac{3}{2} \quad 0 \frac{3}{2}}^{3=2}(\quad)^2 &= \frac{1}{2}(1+3\cos^2 \quad) \\ X_{0=1}^{\frac{3}{2}} d_{\frac{3}{2} \quad 0 \frac{1}{2}}^{3=2}(\quad)^2 &= \frac{3}{2}\sin^2 \quad : \end{aligned} \quad (48)$$

In figure 2 we plot the spin relaxation time τ_{sp} of the heavy- and light-hole excitons as functions of the exciton wavevector K in GaS/Al_{0.3}Ga_{0.7}As quantum wells of

well width 70 Å and lattice temperature $T_{\text{lat}} = 10$ K. We calculate τ_{sp} corresponding to intraband scatterings of heavy-hole to heavy-hole (labelled HH \rightarrow HH) due to the deformation potential interaction using equations (32), (35), (40), (44), (45) and (47) and integrating over both the in-plane (q_{\parallel}) and perpendicular (q_{\perp}) components of the phonon wavevector. A similar approach is used to calculate τ_{sp} due to light-hole to light-hole scattering (LH \rightarrow LH) via the deformation potential interaction. τ_{sp} due to the decay of the heavy-hole exciton (HH \rightarrow e + h) and decay of light-hole exciton (LH \rightarrow e + h) is likewise calculated using equations (32), (35), (40), (44) and (45) and the appropriate transition matrix elements. The material parameters used in the calculation (following [7], [51]–[55]) are listed in table 1. We employ the BenDaniel-Hukemodell [34] and the approach outlined in the Appendix to calculate the electron and hole wavefunctions $\psi_{e,j}(z_e)$ and $\psi_{h,j}^z(z_h)$ respectively. We have assumed $\epsilon_{\text{TA1}} = \epsilon_{\text{TA2}}$ and have neglected the effective mass and dielectric mismatches between the well and barrier materials in our calculations.

Our results show that as the wavevector K increases, the exciton spin relaxation is likely to occur via the decay channel rather than by the scattering mechanism. Depending on K , the heavy-hole and light-hole excitons assume different roles under the scattering and decay processes. The light-hole exciton is more likely to decay (at large K) while the heavy-hole exciton is more likely to be scattered (at small K) during spin relaxation. It is interesting to note that the estimated times for τ_{sp} are reasonably close for the decay and scattering mechanisms in the range $3 \times 10^7 \text{ m}^{-1} \leq K \leq 6.5 \times 10^7 \text{ m}^{-1}$. This indicates the delicate balance between decay and scattering processes which gives rise to spin relaxation mechanisms and the need for a careful examination of the effect of the exciton temperature T_{ex} and the exciton density n_{ex} on exciton spin dynamics in low dimensional systems.

While LA and TA phonons are both effective in bringing about spin relaxation, the contribution from TA phonons appears to dominate the spin dynamics of excitons for a wide range of K . The spin relaxation times (via the scattering and decay processes) are calculated to be of the order of 10 to 100 ps which is consistent with experimental results [9, 10] measuring τ_{sp} in the order of a 100 picoseconds. In table 2 we have compared τ_{sp} (ps) corresponding to various scattering processes in GaAs/Al_{0.3}Ga_{0.7}As quantum wells at well width 100 Å, $K = 2 \times 10^7 \text{ m}^{-1}$ and $T_{\text{lat}} = 4.2$ K. The calculated values show that spin relaxation is dominated by TA phonons coupled via the piezoelectric interaction to excitons undergoing intraband (HH \rightarrow LH) scattering.

In figure 3 we plot the spin transition time τ_{sp} as a function of dimensionality of the heavy-hole exciton in GaAs/Al_{0.3}Ga_{0.7}As material systems. The contribution of both LA and TA phonons is included in the decay and intraband scattering calculations in which only the deformation potential interaction is taken into account. Figure 3 shows clearly the explicit dependence of τ_{sp} on d . It is interesting to note that τ_{sp} rises as high as 1×10^3 ps (1×10^6 ps for $d = 1.3$). Experimental results [16] have shown that the spin relaxation time of excitons in quantum disks is much higher (~ 1000 ps) than in quantum wells. Hence at small dimensionalities there is a substantial increase in τ_{sp} . In table 3 we have compared τ_{sp} due to the deformation potential interaction for different configurations of GaAs/Al_{0.3}Ga_{0.7}As systems. The results show the striking effect on τ_{sp} of changing the radius of both the quantum wire and the quantum disk and its thickness.

Fig. 2

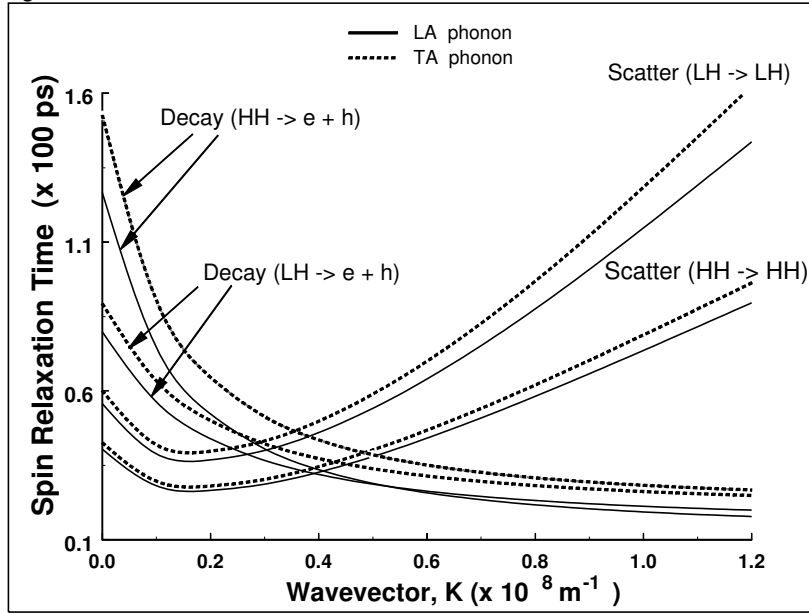


Figure 2. The spin transition time τ_{sp} as a function of the exciton wavevector K in $\text{GaAs}/\text{Al}_{0.3}\text{Ga}_{0.7}\text{As}$ quantum wells. τ_{sp} involves intraband scatterings of heavy-hole to heavy-hole (labelled as HH \rightarrow HH) and light-hole to light-hole scattering (LH \rightarrow LH), and decay of the heavy-hole exciton (HH \rightarrow e + h) and light-hole exciton (LH \rightarrow e + h). The temperatures are $T_{\text{lat}} = 10$ K and $T_{\text{ex}} = 20$ K.

Fig. 3

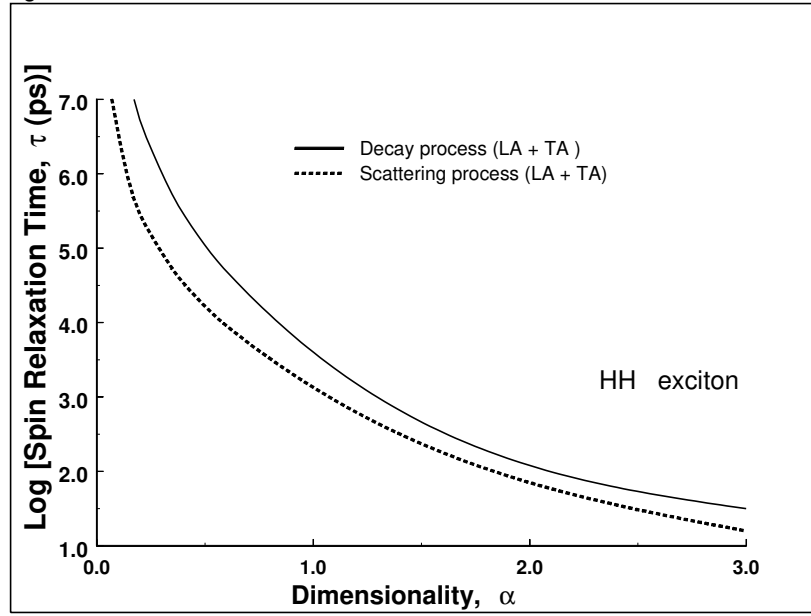


Figure 3. Spin transition time τ_{sp} as a function of the dimensionality of the heavy-hole exciton in the GaAs/Al_{0.3}Ga_{0.7}As material system at $K = 1 \cdot 10^7 \text{ m}^{-1}$ and $T_{\text{lat}} = 4.2 \text{ K}$, $T_{\text{ex}} = 20 \text{ K}$. All other parameters used are listed in table 1. The contribution of both LA and TA phonons are included in the decay and intraband scattering calculations.

Table 1. Material parameters.

	5318	10^3 kg/m^3		12.9	1	6.85
T_A	186	10^3 m/s	a	0.31 eV	2	2.1
T_{LA}	425	10^3 m/s	b	2.86 eV	3	2.9
\hbar_{14}	0.16	C/m^2	c	2.27 eV	g	4
ϵ_c	8.0	eV	T_{ex}	20 K	n_{ex}	$5 \cdot 10^9 \text{ cm}^{-2}$

Table 2. Comparison of τ_{sp} (ps) corresponding to various scattering processes in GaAs/Al_{0.3}Ga_{0.7}As quantum well at well width 100 Å, $\mathcal{K} = 2 \cdot 10^7 \text{ m}^{-1}$, with $T_{lat} = 4.2 \text{ K}$, $T_{ex} = 20 \text{ K}$.

	Deform (LA)	Deform (TA)	Piezo (LA)	Piezo (TA)
HH ! HH	23	26	35	44
LH ! LH	34	38	49	58
HH LH	48	63	70	79

Table 3. Comparison of τ_{sp} of the heavy-hole exciton due to the deformation potential interaction for different configurations of GaAs/Al_{0.3}Ga_{0.7}As systems at $\mathcal{K} = 1 \cdot 10^7 \text{ m}^{-1}$ with $T_{lat} = 4.2 \text{ K}$, $T_{ex} = 20 \text{ K}$. Other parameters used are listed in table 1.

	Radius R (Å)	Thickness L (Å)	Dimensionality	τ_{sp} (ps) HH ! HH (Scat)	τ_{sp} (ps) HH ! e+h (Decay)
quantum wire	50	–	1.31	450	$1 \cdot 10^3$
quantum wire	100	–	1.93	82	150
quantum disk	30	50	0.85	$2.7 \cdot 10^3$	$1.1 \cdot 10^4$
quantum disk	100	100	1.72	135	223
quantum disk	300	150	2.24	50	83

7. Conclusions

We have performed a comprehensive investigation of exciton spin relaxation involving LA and TA acoustic phonons for various configurations of the GaAs/Al_{0.3}Ga_{0.7}As material system. Our results show the explicit dependence of τ_{sp} on \mathcal{K} which is an important result as the relative motion of an exciton is possibly best described by an intermediate dimension in quantum wells, wires or disks. Our results also highlight the specific role played by TA phonons coupled via the piezoelectric interaction to excitons. Our calculations show good agreement with experimental measurements and can be easily extended to coupled double quantum wells as well as to indirect excitons and impurities confined in low dimensional systems. Our results show that depending on the exciton centre-of-mass wavevector, the balance between decay and scattering mechanisms resulting in exciton spin relaxation can be delicate. Future developments in this field of research will therefore require a careful examination of the conditions (for example the exciton temperature, density and configuration) before an accurate picture can be drawn of the spin dynamics of excitons in semiconductor systems.

8. Appendix

The hole wavefunction can be written as a superposition of four states of the valence band top (labelled by $m = \pm \frac{3}{2}; \pm \frac{1}{2}$), characterized by the Luttinger parameters $\gamma_1; \gamma_2$ and γ_3 which appear in the 4×4 Luttinger Hamiltonian [28]:

$$\hat{H}_c = \begin{pmatrix} 0 & c & b & 0 \\ c & H_{hh} & 0 & b \\ b & 0 & H_{lh} & c \\ 0 & b & c & H_{hh} \end{pmatrix} + V_h(z_h; L_w) I_4; \quad (49)$$

where I_4 is the 4×4 identity matrix and where the heavy-hole and light-hole Hamiltonians $H_{hh}; H_{lh}$ and the mixing parameters are given by

$$\begin{aligned} H_{hh} &= \frac{1}{2m_0} \hbar^2 k_{zh}^2 \left(\gamma_1 - \frac{\gamma_2}{2} \right) - \frac{\hbar^2 (k_x^2 + k_y^2)}{2m_0} \left(\gamma_1 + \frac{\gamma_2}{2} \right) \\ H_{lh} &= \frac{1}{2m_0} \hbar^2 k_{zh}^2 \left(\gamma_1 + \frac{\gamma_2}{2} \right) - \frac{\hbar^2 (k_x^2 + k_y^2)}{2m_0} \left(\gamma_1 - \frac{\gamma_2}{2} \right) \\ c(k_x; k_y) &= \frac{\hbar^2}{3} \frac{\gamma_3}{2m_0} (k_x - ik_y)^2 \\ b(k_x; k_y; p_{zh}) &= \frac{\hbar^2}{3} \frac{\gamma_3}{2m_0} \hbar p_{zh} i(k_x - ik_y); \end{aligned}$$

where m_0 is the free-electron mass and $V_h(z_h; L_w)$ is the square well potential of thickness L_w that confines the holes. $\mathbf{k}_h = (k_{xh}; k_{yh}; k_{zh})$ denotes the three-dimensional wavevector of the holes. We have also used the axial approximation $\gamma_2 = \gamma_3$ to simplify $c(\mathbf{k}_h)$ to a single term and have replaced k_{zh} by $i\partial/\partial z_h$ in the expression for $\hbar^2 k_{zh}^2$. The material parameters $\gamma_1; \gamma_2; \gamma_3$ are related to the inverse effective masses of electrons and holes. In the k_{zh} direction the heavy-hole, light-hole masses are given by, respectively,

$$m_{hh} = \frac{1}{\gamma_1 - \frac{\gamma_2}{2}}; \quad m_{lh} = \frac{1}{\gamma_1 + \frac{\gamma_2}{2}};$$

The transverse masses of the charge carriers are given by the coefficients of the $k_x^2 + k_y^2$ terms. Consequently the light-hole transverse mass is larger than the heavy-hole transverse mass.

The hole wavefunctions in a quantum well are obtained by solving:

$$\sum_{\frac{0}{2}} \langle \mathbf{h}_z | \hat{H}_c | \mathbf{j}_z \rangle + V_h(z_h; L_w) \psi_{\mathbf{k}_h}^z(z_h) = E_h(\mathbf{k}_h) \psi_{\mathbf{k}_h}^z(z_h) \quad (50)$$

where the hole energy $E_h(\mathbf{k}_h)$ corresponds to a heavy-hole or light-hole, depending on the mass used to model the profile of the potential function $V_h(z_h)$. The summation is over the four spin projections $\frac{0}{2} = \pm \frac{3}{2}; \pm \frac{1}{2}$ of the hole spin, with $\frac{0}{2}$ aligned along the quantization axis. When $b = c = 0$ the Hamiltonian \hat{H}_c splits into two independent Hamiltonians, one each for the heavy-hole ($\frac{0}{2} = \pm \frac{3}{2}$) and light-hole ($\frac{0}{2} = \pm \frac{1}{2}$) cases.

References

- [1] Weisbuch C and Vinter B 1991 Quantum Semiconductor Structures (Boston: Academic)

- [2] Haug H and Koch S W 1993 *Quantum Theory of the Optical and Electronic Properties of Semiconductors* (Singapore: World Scientific)
- [3] Shah J 1999 *Ultrafast Spectroscopy of Semiconductors and Semiconductor Nanostructures*, Springer Series in Solid-State Sciences (Berlin: Springer-Verlag) vol 115
- [4] Maialle M Z, de Andrade Silva E A and Sham L J 1993 *Phys. Rev. B* 47 15776{88}
- [5] Oh IK, Singh J, Thilagam A and Vengurlekar A S 2000 *Phys. Rev. B* 62 2045{50}
- [6] Soroko A V and Ivanov A L 2002 *Phys. Rev. B* 65 165310
- [7] Ivanov A L, Littlewood P B and Haug H 1999 *Phys. Rev. B* 59 5032{48}
- [8] Meier F and Zakharchenya B P 1984 *Optical Orientation* (Amsterdam: North-Holland)
- [9] Damen T C, Leo K, Shah J, and Cunningham J E 1991 *Appl. Phys. Lett.* 58 1902{4}
- [10] Munez L, Perez E, Vina L and Ploog K 1995 *Phys. Rev. B* 51 4247{57}
- [11] Wolf S A, Awschalom D D, Buhrman R A, Daughton J M, von Molnar S, Roukes M L, Chtchelkanova A Y and Treger D M 2001 *Science* 294 1488{95}
- [12] Buyanova I A, Chen W M, Toropov A A, Sorokin S V, Ivanov S V and Kop'ev P S 2003 *Journal of Superconductivity* 16 399{402}
- [13] Pikus G E and Titkov A N 1984 *Optical Orientation* ed Meier F and Zakharchenya B P (Amsterdam: North-Holland)
- [14] Maialle M Z 1998 *Semiconductor Science and Technology* 13 852{7}
- [15] Ueno Yamata T and Sham L J 1990 *Phys. Rev. B* 42 7114{23}
- [16] Gotoh H, Ando H, Kamada H, Chavez-Pirson A and Tammyo J 1998 *Appl. Phys. Lett.* 72 1341{3}
- [17] Vinattieri A, Shah J, Damen T C, Goossen K W, Pfeiffer L N, Maialle M Z and Sham L J 1993 *Appl. Phys. Lett.* 63 3164{6}
- [18] Snoke D W, Ruhle W W, Kohler K and Ploog K 1997 *Phys. Rev. B* 55 13789{94}
- [19] Dresselhaus G 1956 *J. Phys. Chem. Solids* 1 14{22}
- [20] Baldeschia A and Lipari N O 1971 *Phys. Rev. B* 3 439{51}
- [21] Lipari N O and Baldeschia A 1971 *Phys. Rev. B* 3 2497{503}
- [22] Kane E O 1975 *Phys. Rev. B* 11 3850{9}
- [23] Rossler U and Trebin H R 1981 *Phys. Rev. B* 23 1961{70}
- [24] Beni G and Rice T M 1977 *Phys. Rev. B* 15 840-3
- [25] Siarkos A, Runge E and Zimmermann R 2000 *Phys. Rev. B* 61 10854{67}
- [26] Rudin S and Reinecke T L 2002 *Phys. Rev. B* 66 85314
- [27] Kane E O 1966 *Semiconductors and Semimetals* ed Willardson R K and Beer A C (New York: Academic Press)
- [28] Luttinger J M 1956 *Phys. Rev.* 102 1030{41}
- [29] Altarelli M, Ekenberg U and Fasolino A 1985 *Phys. Rev. B* 32 5138{43}
- [30] Broido D A and Sham L J 1986 *Phys. Rev. B* 34 3917{23}
- [31] Edmunds A R 1957 *Angular Momentum in Quantum Mechanics* (Princeton, NJ: Princeton University Press)
- [32] Brink D M and Satchler C R 1962 *Angular Momentum* (Oxford: Clarendon Press)
- [33] Biedenharn L C and Louck J D 1981 *Angular Momentum in Quantum Physics Encyclopedia of Mathematics and its Applications* vol 8 (Reading, MA: Addison-Wesley)
- [34] Bendaniel D J and Duke C B 1966 *Phys. Rev.* 152 683{92}
- [35] Bayer M, Ortner G, Stern O, Kuther A, Gorbunov A A, Forchel A, Hawrylak P, Fafard S, Hinz K, Reinecke T L, Walck S N, Reithmaier J P, Klotz F and Schäfer F 2002 *Phys. Rev. B* 65 195315
- [36] Winkler R 1995 *Phys. Rev. B* 51 14395{409}
- [37] Thilagam A and Singh J 1993 *J. Lumin.* 55 11{6}
- [38] Thilagam A 2001 *Phys. Rev. B* 63 045321
- [39] Thilagam A 1997 *Phys. Rev. B* 56 4665{70}
- [40] Tanguy C, Lefebvre P, Mathieu H and Elliot R J 1997 *J. Appl. Phys.* 82 798{802}
- [41] Thilagam A and Matos-Abiad A 2004 *J. Phys.: Condens. Matter* 16 3981{4000}
- [42] Thilagam A 1997 *Phys. Rev. B* 56 9798{804}
- [43] Karlsson K F, Dupertuis M A, Wemman H and Kapon E 2004 *Phys. Rev. B* 70 153306
- [44] Lohe M A and Thilagam A 2004 *J. Phys. A: Math. Gen.* 37 6181{99}
- [45] Christol P, Lefebvre P and Mathieu H 1993 *J. Appl. Phys.* 74 5626{37}
- [46] Mikhailov I D, Betancur F J, Escorcia R A and Sierra-Ortega J 2003 *Phys. Rev. B* 67 115317
- [47] Matos-Abiad A, Oliveira L E and de Dios-Leyva M 1998 *Phys. Rev. B* 58 4072{6}
- [48] Ehrenreich H and Overhauser A W 1956 *Phys. Rev.* 104 331{42}
- [49] Gantmakher V F and Levinson Y B 1987 *Carrier Scattering in Metals and Semiconductors* (Amsterdam: North-Holland)

- [50] Besombes L, Kheng K, Marsall L and Mariette H 2001 Phys. Rev. B 63 155307
- [51] Bir G L and Pikus G E 1975 Symmetry and Strain-Induced Effects in Semiconductors (New York: Wiley)
- [52] Ivchenko E L and Pikus G E 1997 Superlattices and Other Heterostructures. Symmetry and Optical Phenomena (Berlin: Springer)
- [53] Gerlich D 1967 J. Phys. Chem. Solids 28 2575{9
- [54] Adachi S 1984 GaAs and Related Materials: Bulk Semiconducting and Superlattice Properties (Singapore: World Scientific)
- [55] Madelung O, Schultz M and Weiss H 1982 Numerical Data and Functional Relationships in Science and Technology vol.17 (Berlin: Springer-Verlag)